



## Research Article

# Identification and validation of protein biomarkers for predicting gastrointestinal stromal tumor recurrence

Juan Sun<sup>1</sup>, Jie Li<sup>1</sup>, Yixuan He, Weiming Kang\*, Xin Ye\*

Department of General Surgery, Peking Union Medical College Hospital, Chinese Academy of Medical Sciences and Peking Union Medical College, Beijing, China

## ARTICLE INFO

## Keywords:

Gastrointestinal stromal tumor  
Recurrence  
Protein biomarkers  
Mass spectrometry  
Immunohistochemistry

## ABSTRACT

We conducted a proteomic analysis using mass spectrometry to identify and validate protein biomarkers for accurately predicting recurrence risk in gastrointestinal stromal tumors (GIST) patients, focusing on differentially expressed proteins in metastatic versus primary GIST tissues. We selected five biomarkers—GPX4, RBM4, TPM3, PFKFB2, and PGAM5—and validated their expressions in primary tumors of recurrent and non-recurrent GIST patients via immunohistochemistry. Our analysis of the association between these biomarkers with recurrence-free survival (RFS) and overall survival (OS), along with their interrelationships, revealed that immunohistochemistry confirmed significantly higher expressions of these biomarkers in primary GIST tissues of recurrent patients. Kaplan-Meier survival analysis showed that high expressions of GPX4, RBM4, TPM3, PFKFB2, and PGAM5 correlated with lower RFS, and GPX4 and RBM4 with lower OS. All biomarker pairs showed positive associations, with high expressions correlating with increased recurrence rates, and GPX4 and RBM4 with higher mortality rates. In conclusion, the biomarkers GPX4, RBM4, TPM3, PFKFB2, and PGAM5 are clinically relevant for predicting GIST recurrence, with their high expressions in primary tumors linked to poorer RFS and OS. They serve as potential prognostic indicators, enabling early treatment and improved outcomes. The observed interrelationships among these biomarkers further validate their accuracy in predicting GIST recurrence.

## 1. Introduction

Gastrointestinal stromal tumors (GISTs) are the most common soft-tissue sarcomas, predominantly arising from the precursor cells of the interstitial cells of Cajal (ICC), which serve as the gastrointestinal tract's pacemaker cells [1]. GISTs constitute a diverse group of tumors marked by distinct activating mutations in oncogenes, mainly KIT (80 %) or PDGFRA (15 %) [2]. The global annual incidence of GISTs varies, with 6 to 22 cases per million individuals reported [3]. The median age of diagnosis is around 65 years [1], and initial symptoms often include bleeding, pain, weight loss, or obstruction. Approximately 60–65 % of GISTs originate in the stomach, and 20–25 % in the small intestine [1]. They are frequently discovered incidentally during CT scans or endoscopic procedures and tend to develop in the submucosa [4], making preoperative pathological biopsy challenging. It's crucial to consider the type, location, and extent of the tumor when deciding on the need for a biopsy [5,6].

The definitive diagnosis of GISTs relies on pathological morphology and immunohistochemical analysis [7]. For incidental small GISTs (<2

cm) found during endoscopy, resection is not typically advised unless they are located in the rectum. However, larger localized GISTs (>2 cm) necessitate complete surgical removal as the primary treatment [1,8]. Despite surgical removal, 15–50 % of patients with GISTs have metastatic disease at diagnosis [9] and the risk of postoperative recurrence and metastasis critically affects prognosis for patients with localized or resectable GIST [10]. Consequently, several risk stratification systems, including the modified National Institutes of Health (NIH) classification [11], Armed Forces Institute of Pathology (AFIP) criteria [7], and National Comprehensive Cancer Network (NCCN) guidelines, have been developed to evaluate the risk of postoperative recurrence [10] based on factors like tumor size, location, mitotic rate, and rupture status [1]. Patients at high risk according to the modified NIH criteria, undergoing only surgical treatment, face a recurrence risk above 50 % [12]. However, accurately assessing recurrence risk in GIST patients is challenging due to the tumor's intrinsic variability and the limitations of biopsy samples [13,14]. Thus, there's a pressing need to identify protein biomarkers that can accurately predict early-stage recurrence risk.

In this study, we conducted proteomic analysis using mass

\* Corresponding authors.

E-mail addresses: [kangwm@pumch.cn](mailto:kangwm@pumch.cn) (W. Kang), [yexinpumch@163.com](mailto:yexinpumch@163.com) (X. Ye).

<sup>1</sup> These authors have contributed equally to this work.

spectrometry to identify proteins with differential expression profiles between primary GIST tumors and their corresponding metastatic sites. We selected five markers for validation in recurrent and non-recurrent GIST patients and examined their association with recurrence-free survival (RFS) and overall survival (OS). Additionally, we evaluated the correlation between these markers to assess their predictive accuracy for recurrence (Fig. 1). By identifying protein biomarkers that can more precisely and earlier predict GIST recurrence, our goal is to pinpoint high-risk patients for early intervention, potentially improving their RFS or OS.

## 2. Methods and materials

### 2.1. Tissue specimen collection

For mass spectrometry analysis, we collected three pairs of primary and metastatic GIST tumor samples, which were diagnosed concurrently. Additionally, 23 primary GIST samples from recurrent patients and 25 from non-recurrent patients were acquired for immunohistochemical (IHC) validation of selected proteins. All specimens were sourced from paraffin-embedded archives at Peking Union Medical College Hospital (PUMCH), with the collection approved by the institutional review board (Reference number: K22C0484).

### 2.2. LC-MS/MS (liquid chromatography tandem-mass spectrometry) proteomics and data processing

Sliced tissues were dewaxed and proteins were extracted with lysis buffer (6 M urea and 2 M thiourea). Protein lysates were reduced with DTT at 95 °C for 5 min, then alkylated with IAM in the dark at room temperature for 45 min. Proteins were loaded onto 10KDa ultracentrifuge tube for FASP digestion. Trypsin digestion was performed overnight at a protein-to-trypsin ratio (w/w) of 50:1. The digested peptides were

desalted using a C18 Ziptip and vacuum-dried. Then, the peptides were resolved and spiked with internal peptide, then delivered to LC-MS/MS system. Peptides were separated by EASY-n LC1000 system (Thermo scientific). The analytical reverse phase column is 25 cm\*50 μm ID (Shimadzu) at a flow rate of 800 nL/min for 45 min with a temperature of 60 °C. The elution gradient is from 4 % to 16 % for 24 min and from 16 % to 24 % for 11 min (buffer A: 0.1 % formic acid, buffer B: 80 % acetonitrile, 0.1 % formic acid). Eluted peptides were analyzed with Orbitrap Fusion Lumos Tribrid instrument (Thermo scientific) with DIA (Data Independent Acquisition) mode. Peptides were ionized at a potential of 2.3 kV. Acquisition parameters included the full scan range of 350 to 1300m/z, charge states of 2 to 5, and a resolution of 60,000 in the Orbitrap using an AGC target value of 1e6 and maximum injection time of 50 msec. The MS/MS were 40 scans after the full MS scan with resolution of 3000. The collision energy was 32 %.

Spectronaut (version 16, Biognosys) was used for protein identification and quantification. The raw files were searched against the Human database downloaded from Swissprot containing 20387 sequences. Tolerance for MS and MS/MS were 10 ppm and 0.02 Da, respectively. The maximum two missed cleavages were allowed. Carbamidomethylation (C) was set as fixed modifications. Oxidation (M) and deamidation were set as variable modifications. Decoy items were generated by inverse mode. False positive rate (FDR) was set as 1 % at the protein and peptide levels. The samples were quantitative evaluation basing on the library-free directDIA. Cross runs were normalized according to the global abundance area. The Fold Change > 2 and p-value < 0.05 were used to determine whether the expression differed significantly [15,16].

### 2.3. Immunohistochemistry (IHC)

The paraffin-embedded tumor tissues were sectioned to a thickness of 4 μm and then the sections were deparaffinized using xylene and rehydrated through a series of graded alcohol solutions. To block endogenous peroxidase activity and minimize non-specific staining, the tissue sections were treated with 3 % H<sub>2</sub>O<sub>2</sub> for 10 min at room temperature to ensure a clean background for subsequent staining. For protein visualization, the tissue sections were subjected to the streptavidin peroxidase-conjugated method. For protein visualization, the tissue sections were subjected to the streptavidin peroxidase-conjugated method. Sections were incubated with the primary antibodies to specifically bind to target proteins within the tissue. The information of primary antibodies is listed as follows: GPX4 (Proteintech 67763-1-Ig), RBM4 (Affinity DF12225), TPM3 (Affinity DF6338), PFKFB2 (Immunoway YP1872), PGAM5 (Proteintech 28445-1-AP). The primary antibodies were utilized and diluted as per the recommended guidelines provided by the manufacturers. Five random fields were selected for analysis under a 40 × objective lens. Image-Pro Plus software was then employed to quantitatively assess the expression levels of the proteins of interest, enabling accurate calculations and providing reliable data for further analysis and interpretation.

### 2.4. Statistical analysis

Statistical analyses were conducted with Graphpad Prism 8.0 (CA, USA) and SPSS 27 (Chicago, USA). Continuous variables were analyzed by calculating the means ± standard deviations (SDs) and compared between groups using unpaired two-tailed t-tests. Categorical variables were summarized using counts and percentages, and group differences were examined using Pearson's  $\chi^2$  test. Patient data were censored at the last follow-up, with RFS and OS time-to-event endpoints for those not experiencing death or recurrence also censored at this time. RFS and OS were modeled using the Kaplan-Meier method with log-rank (Mantel-Cox) testing to compare patient groups. Pearson's correlation analysis assessed the predictive interrelationships of five proteins for GIST recurrence. Differences between groups were considered significant at

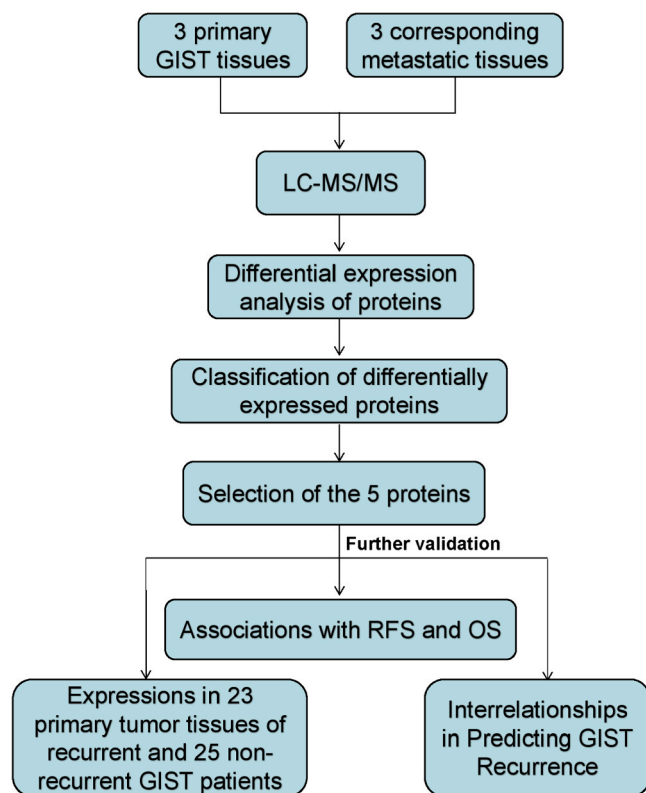


Fig. 1. Schematic workflow representation of our study based on LC-MS/MS in GIST tissues.

P-value of  $< 0.05$ . (\* $P < 0.05$ , \*\* $P < 0.01$ , \*\*\* $P < 0.001$ ).

### 3. Results

#### 3.1. Differential expression analysis of proteins in primary tumor tissues and the corresponding metastatic tissues of GIST patients using LC-MS/MS-based quantitative proteomics

We collected and analyzed tissue specimens from three GIST patients, covering both metastatic and primary GIST tissues, which were diagnosed concurrently. A total of 4542 proteins were identified, and quantitative analysis was performed on 3283 proteins with 2 peptides. Missing values were imputed using half of the minimum protein value. Differentially expressed proteins were selected based on a  $\log_2$  (Fold Change)  $> 2$  and a p-value  $< 0.05$ . Ultimately, we identified 36 proteins with significantly higher expression in metastatic tissues (Supplementary Material). We excluded the gene GGT from further analysis because all metastatic GIST tissues originated from the liver and GGT is associated with liver function. Then we selected the top three genes (GPX4, TPM3, PGAM5) for validation. To align with literature and enhance validation, we selected two genes, RBM4 and PFKFB2, for further study due to their high  $\log_2$  (Fold Change) and low p-values (Fig. 2). The detected peptide sequences of them were: GPX4: ILAFPCNQFGK, YGP-MEEPLVIEK; TPM3: KLVIIEGDLER; PGAM5: AIETTDIISR, REPLSLINVR; RBM4: VLECDIIK, ATAPVPTVGEQYGYGHESELSQASAAAR; PFKFB2: LEPVIMELER, HGESEFNLLGK.

#### 3.2. Classification of differentially expressed proteins

Using the PANTHER (Protein Analysis Through Evolutionary Relationships) Classification System, we systematically categorized 36 differentially expressed proteins, enhancing our understanding of their molecular and functional characteristics. After removing unclassified proteins, we classified the remaining proteins into seven molecular functions, two cellular components, and ten biological processes (Fig. 3). Binding (53.4 %) and catalytic activity (23.3 %) emerged as the top molecular function categories. Two cellular components were identified: cellular anatomical entity (77.8 %) and protein-containing complex (22.2 %). The biological process analysis predominantly involved upregulated proteins in cellular processes (32.9 %), localization (17.2 %), metabolic processes (15.5 %), and biological regulation (13.8 %). Among the five selected proteins, TPM3, RBM4, and PFKFB2 were associated with specific Gene Ontology terms, while GPX4 and

PGAM5 were not classified by PANTHER. Specifically, TPM3, RBM4, and PFKFB2 were linked to the GO:0110165 cellular anatomical entity and GO:0009987 cellular processes. For molecular function, TPM3 and RBM4 were classified under GO:0005488 (binding), and PFKFB2 under GO:0003824 (catalytic activity). Utilizing this classification system provided valuable insights into the complex roles of these proteins in cellular processes.

#### 3.3. Validation of expression of 5 proteins in primary tumor tissues of recurrent and non-recurrent GIST patients

To explore the roles of selected five proteins in GIST recurrence, we analyzed primary tissue specimens from 23 recurrent and 25 non-recurrent GIST patients. The clinical and pathological characteristics of these 48 patients are summarized in Table 1. RFS was significantly lower in the recurrent group than in the non-recurrent group. Furthermore, the recurrent group exhibited a higher mortality rate. Higher IOD levels in GPX4, RBM4, TPM3, PFKFB2, and PGAM5 were linked to increased recurrence rates. Baseline factors including age, BMI, inpatient days, sex, surgery method, tumor size, tumor site, mitotic index, and recurrence risk showed no significant differences between the two groups. Immunohistochemical staining revealed significantly higher expression of the five proteins in primary GIST tissues of recurrent patients than in non-recurrent patients (Fig. 4). This suggests the proteins are crucial in GIST recurrence, potentially serving as biomarkers for prediction.

#### 3.4. Association of differentially expressed proteins with recurrence-free survival and overall survival in GIST patients

To validate the clinical impact of five proteins on GIST recurrence, we conducted a follow-up study with 48 patients to assess their RFS and OS. We used Kaplan-Meier survival analysis to evaluate the association of the five proteins with patient survival outcomes. Results showed a significant decrease in RFS for GIST patients with high levels of GPX4, RBM4, TPM3, PFKFB2, and PGAM5. However, only high expression levels of GPX4 and RBM4 were significantly associated with reduced OS, with no significant associations observed for the other proteins (Fig. 5). These findings underscore the clinical significance of these five proteins in predicting GIST recurrence, linked to poorer RFS at high expression levels. Their predictive accuracy for OS, however, is inconsistent.

#### 3.5. Interrelationships of 5 Proteins in Predicting GIST Recurrence

The results clearly show that the five biomarkers are significantly relevant for predicting GIST recurrence, with consistent outcomes. Consequently, we analyzed the correlation of IOD levels for the five proteins among the 48 patients. Pearson correlation analysis showed a moderate positive correlation between each protein pair (Fig. 6). Furthermore, we statistically analyzed the clinical and pathological data of the 48 patients based on the expression levels of GPX4, RBM4, TPM3, PFKFB2, and PGAM5, as illustrated in Table 2. Patients with high expression levels of all five proteins showed significantly higher GIST recurrence rates than those with low expression levels. However, only GPX4 and RBM4 exhibited statistically significant differences in mortality rates. The chi-square test, applied after grouping protein expressions, revealed statistical differences in the correlations among GPX4 and RBM4, RBM4 and PFKFB2, RBM4 and PGAM5, and TPM3 and PGAM5.

## 4. Discussion

GIST recurrence significantly impacts patient survival, and accurate prediction remains a critical challenge in clinical practice. Our study reveals that GPX4, RBM4, TPM3, PFKFB2, and PGAM5 are significantly relevant in predicting GIST recurrence. Higher expression levels of these

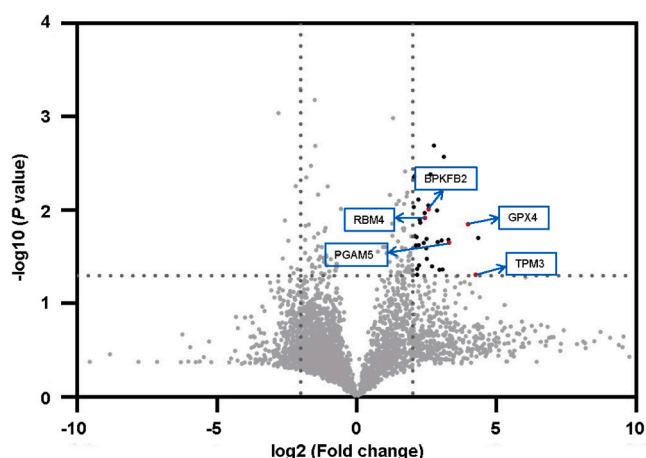


Fig. 2. Volcano plot of differentially expressed proteins (DEPs) between three pairs of primary and metastatic GIST tumor samples. Black dots indicate the upregulated DEPs with a  $\log_2FC > 2$  and  $p < 0.05$ . Among the total of 36 upregulated DEPs, five proteins (marked as red dots) were selected for further analysis.

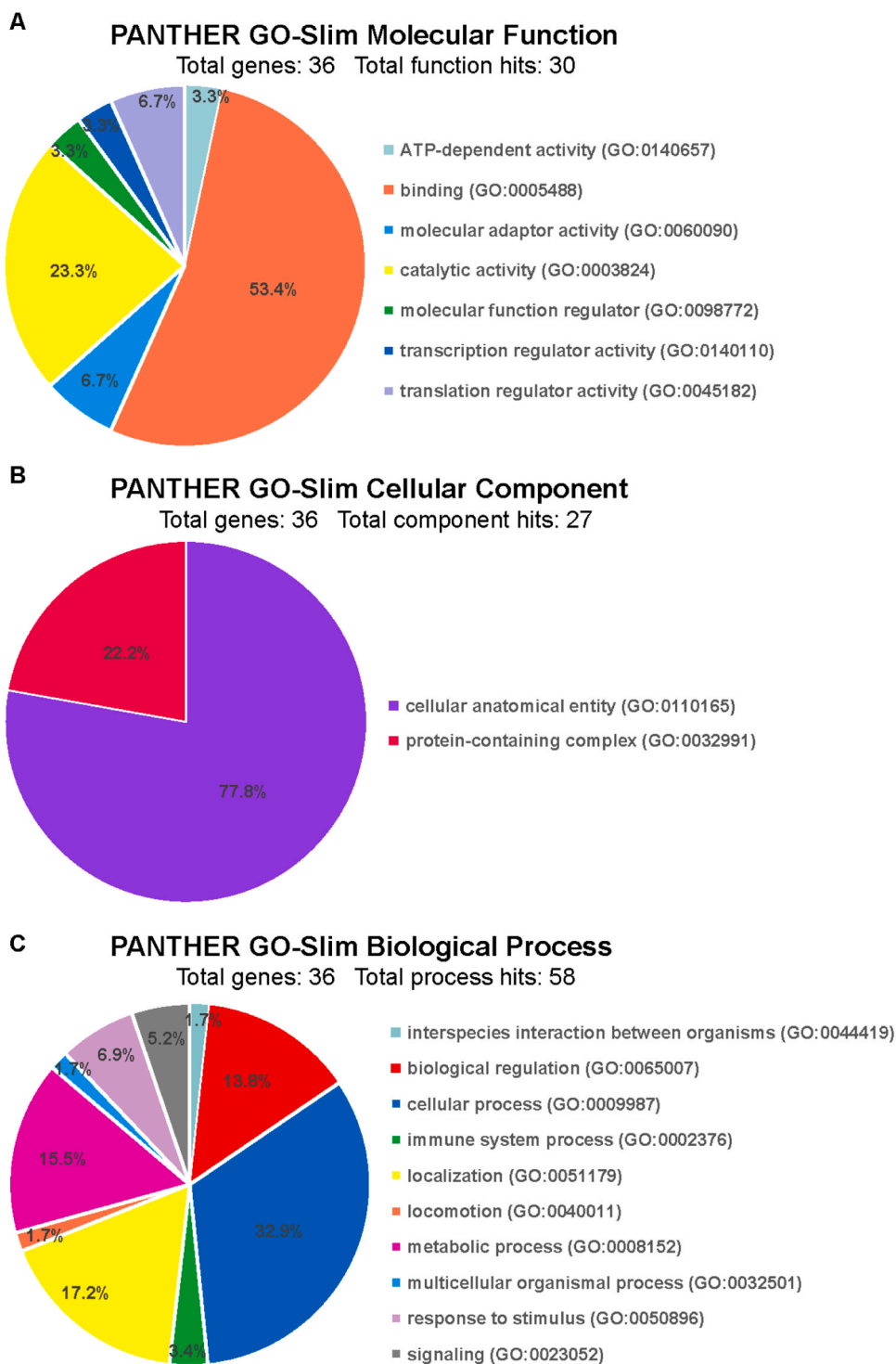


Fig. 3. Classification of the 36 identified proteins by the GO database. (A) Molecular function (B) Cellular component (C) Biological process.

proteins in primary GIST tissues of recurrent patients suggest their potential as biomarkers for predicting recurrence. Furthermore, all proteins are significantly associated with decreased RFS, with only GPX4 and RBM4 significantly affecting OS. Additionally, correlation analysis reveals a positive correlation among these proteins. These findings underscore the clinical value of these biomarkers in predicting GIST recurrence and lay the groundwork for further research into personalized treatment and prognosis in GIST patients.

GISTs, characterized by KIT and/or PDGFRA mutations, have seen median survival times increase from 18 months to over 5 years with the

introduction of tyrosine kinase inhibitors (TKIs) targeting these mutations [6,8]. Despite 3 years of effective adjuvant therapy with imatinib, high-risk patients often relapse within 1–3 years post-treatment, whereas low-risk patients may experience delayed recurrence [8]. Current ESMO guidelines recommend 3 years of adjuvant imatinib therapy for patients with a high relapse risk, emphasizing a shared decision-making process for those with intermediate risk [8,17]. GIST recurrence risk assessment relies mainly on tumor size, mitotic index, location, and the presence of tumor rupture [1]. Recent analysis by Trinh et al. of 19,030 GIST patients from the U.S. National Cancer

**Table 1**

The clinical and pathological characteristics of patients with and without recurrence.

	Recurrent	Non-recurrent	P value
No.	23	25	
Age (years)	57.52 ± 11.21	58.68 ± 11.81	0.730
BMI (kg/m <sup>2</sup> )	22.85 ± 2.74	24.02 ± 3.58	0.214
Inpatient days	14.57 ± 5.55	13.04 ± 4.09	0.281
RFS (month)	34.83 ± 24.97	78.00 ± 23.03	< 0.001***
OS (month)	60.78 ± 32.56	74.80 ± 25.56	0.102
Sex			0.613
Males	15 (65.22 %)	18 (72.00 %)	
Females	8 (34.78 %)	7 (28.00 %)	
Surgery way			0.838
Laparotomy	15 (65.22 %)	17 (68.00 %)	
Laparoscopy	8 (34.78 %)	8 (32.00 %)	
Tumor size (cm)			0.668
> 2, ≤ 5	6 (26.09 %)	4 (16.00 %)	
> 5, ≤ 10	9 (39.13 %)	12 (48.00 %)	
> 10	8 (34.78 %)	9 (36.00 %)	
Tumor site			0.597
Gastric	10 (43.48 %)	9 (36.00 %)	
Non-gastric	13 (56.52 %)	16 (64.00 %)	
Mitotic index (/50 FP)			0.130
≤ 5	7 (30.43 %)	13 (52.00 %)	
> 5	16 (69.57 %)	12 (48.00 %)	
Recurrence risk			0.958
High	18 (78.26 %)	19 (76.00 %)	
Medium	3 (13.04 %)	4 (16.00 %)	
Low	2 (8.70 %)	2 (8.00 %)	
Death			0.003**
Yes	9 (39.13 %)	1 (4.00 %)	
No	14 (60.87 %)	24 (96.00 %)	
IOD of GPX4			0.009**
High	16 (69.57 %)	8 (32.00 %)	
Low	7 (30.43 %)	17 (68.00 %)	
IOD of RBM4			< 0.001***
High	19 (82.61 %)	5 (20.00 %)	
Low	4 (17.39 %)	20 (80.00 %)	
IOD of TPM3			0.009**
High	16 (69.57 %)	8 (32.00 %)	
Low	7 (30.43 %)	17 (68.00 %)	
IOD of PFKFB2			< 0.001***
High	18 (78.26 %)	6 (24.00 %)	
Low	5 (21.74 %)	19 (76.00 %)	
IOD of PGAM5			0.009**
High	16 (69.57 %)	8 (32.00 %)	
Low	7 (30.43 %)	17 (68.00 %)	

Statistical significance was determined by t-test and chi-square test. (\*P < 0.05, \*\*P < 0.01, \*\*\*P < 0.001).

Database suggests the current thresholds for tumor size and mitotic index may be suboptimal. They propose reevaluating these thresholds, suggesting 7 cm for tumor size and a mitotic rate of > 10 per 5 mm<sup>2</sup> for accurate risk stratification [18]. Additionally, a retrospective analysis of 542 gastric GIST patients showed that tumor size, location, and surface ulceration are closely linked to malignant potential [19]. Given these limitations and the variability in risk assessment, identifying protein biomarkers for GIST recurrence prediction is promising. Our study's identified protein biomarkers, with higher expression in recurrent GIST patients' primary tumors, correlate with poorer RFS and OS. Positive correlations among all biomarker pairs further support their predictive accuracy for GIST recurrence. These findings highlight the clinical relevance and prognostic potential of these biomarkers for GIST recurrence. Integrating these biomarkers into current risk assessment models could enhance GIST recurrence risk stratification accuracy and support personalized treatment.

GPX4 (Glutathione Peroxidase 4) is crucial for cellular protection against oxidative damage. It reduces hydrogen peroxide and lipid hydroperoxides, preventing harmful reactive oxygen species (ROS) buildup [20]. GPX4 is involved in cellular processes including ferroptosis, a regulated cell death form dependent on iron and lipid peroxidation [21]. Given that oxidative stress and ROS can influence the tumor

microenvironment, affecting processes like invasion, migration, and angiogenesis, GPX4 has been linked to tumor progression [22,23]. For example, Lu et al. demonstrated that GPX4 inhibition suppresses cell migration and invasion in renal cell carcinoma [24]. Regarding GIST, Ishida et al.'s study showed the GPX4 inhibitor RSL3 induces ferroptotic cell death in both imatinib-sensitive and -resistant GIST cells [25]. Additionally, Delvaux et al. revealed a strong link between GIST risk stratification and transferrin receptor 1 (TFRC) expression levels, essential for iron internalization via receptor-mediated endocytosis [26]. However, research on the relationship between GPX4 and GIST recurrence is still limited.

RBM4 (RNA-Binding Motif Protein 4) is an RNA-binding protein involved in alternative splicing, translation regulation, and RNA stability [27]. Cancer cells can evade senescence and re-enter the cell cycle, promoting malignant spread [28,29]. This process is linked to an active anabolic metabolism that utilizes glucose and glutamine for energy and biosynthesis [30,31]. Chen et al.'s study showed that RBM4 helps esophageal squamous cell carcinoma (ESCC) cells bypass senescence and sustain proliferation by activating glutamine metabolism. They also found that ESCC patients with high RBM4 levels had significantly worse overall survival compared to those with low RBM4 [32]. Furthermore, Han et al.'s study revealed that RBM4 stabilizes RelA/p65 mRNA, enhancing NF-κB signaling and upregulating VEGF-A expression, accelerating angiogenesis in hepatocellular carcinoma (HCC) [33]. RBM4 has also been implicated in the promotion of breast cancer [34]. However, a conflicting report suggests RBM4 may act as a tumor suppressor in lung cancer [35], while another study associates reduced RBM4 levels with poor prognosis in HCC patients undergoing hepatectomy [36]. The variability in these findings may due to the genetic background and tumor heterogeneity [33], and the understanding of the relationship between RBM4 and GIST remains limited, necessitating further investigations.

TPM3 (Tropomyosin 3), a component of the cytoskeleton, is a thin filament protein that supports cell structure and facilitates cell motility [37]. The precise role of TPM3 in tumor biology remains enigmatic. Previous research has shown TPM3 impacts sarcomeric function by reducing Ca<sup>2+</sup> sensitivity and affecting length-dependent Ca<sup>2+</sup> activation [37]. Other studies have found TPM3 involved in thyroid papillary carcinoma and chronic eosinophilic granulocyte leukemia development through fusion with neurotrophic receptor tyrosine kinase 1 and Platelet-derived growth factor receptor β, respectively [38,39]. Yu et al. reported significantly higher TPM3 expression in stage III ESCC tissues than in stage I [40] and Choi et al. demonstrated TPM3 overexpression alters liver cancer cell invasion and metastasis via influencing EMT [41]. Another study showed suppressing TPM3 expression with TPM3-siRNA reduced cellular invasion and migration and decreased MMP-9 and SNAI1 levels in glioma cells [42]. However, research on TPM3's role in GIST is limited, with some exceptions like reported TPM3-NTRK1 fusion cases in mesenchymal spindle-cell neoplasms, distinct from GIST [43, 44].

PFKFB2 (6-Phosphofructo-2-Kinase/Fructose-2,6-Bisphosphatase 2) is an enzyme that regulates glycolysis in eukaryotes [45]. The presence of PFKFB2 expression, linked to cancer's metabolic changes like increased glycolysis for growth advantage, is closely associated with cancer progression [46–48]. For example, Qu et al. demonstrated that circFLNA, upregulated in gastric cancer, promotes cancer proliferation, metastasis, and glycolysis, and inhibits apoptosis by regulating the miR-646/PFKFB2 axis [49]. In HCC, Ji et al. found high MACC1 and PFKFB2 levels associated with TNM stage, Edmondson-Steier classification, and overall survival [50]. Zhao et al. discovered significant PFKFB2 overexpression in metastatic ovarian cancer compared to normal and non-metastatic ovarian cancer [51]. However, the relationship between GIST and PFKFB2 remains unexplored.

PGAM5 (Phosphoglycerate Mutase Family Member 5), an enzyme crucial for cellular energy metabolism, regulates mitochondrial function, cell death pathways, and oxidative stress response [52]. It has been

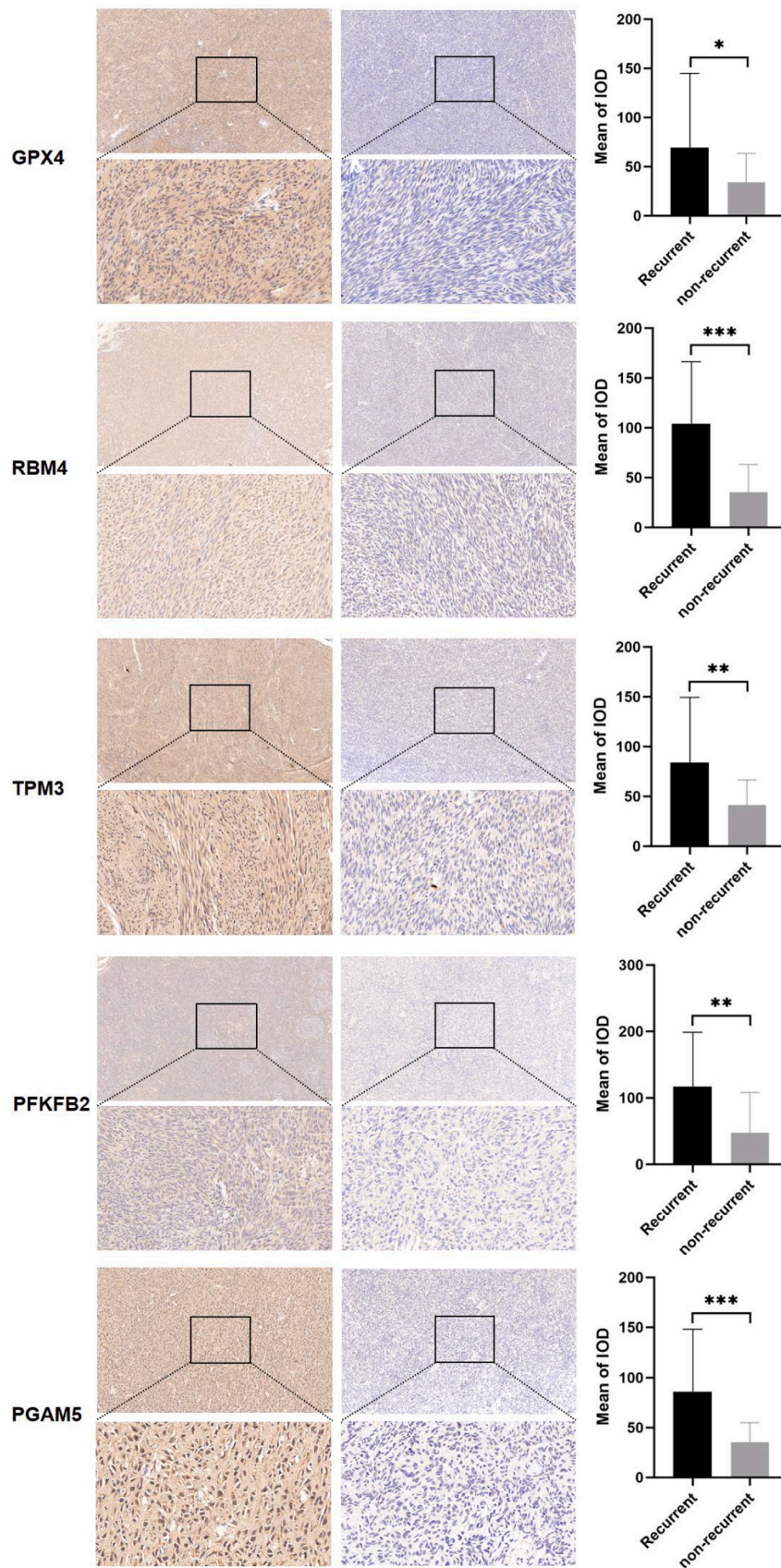


**Fig. 4.** Expressions of GPX4, RBM4, TPM3, PFKFB2, PGAM5 in primary GIST tissues from 23 recurrent and 25 non-recurrent patients. Representative IHC staining (100X and 400X) and quantification of five random fields by mean of integrated optical density (IOD) using Image-Pro Plus in different markers and groups. (\* $P < 0.05$ , \*\* $P < 0.01$ , \*\*\* $P < 0.001$ ).

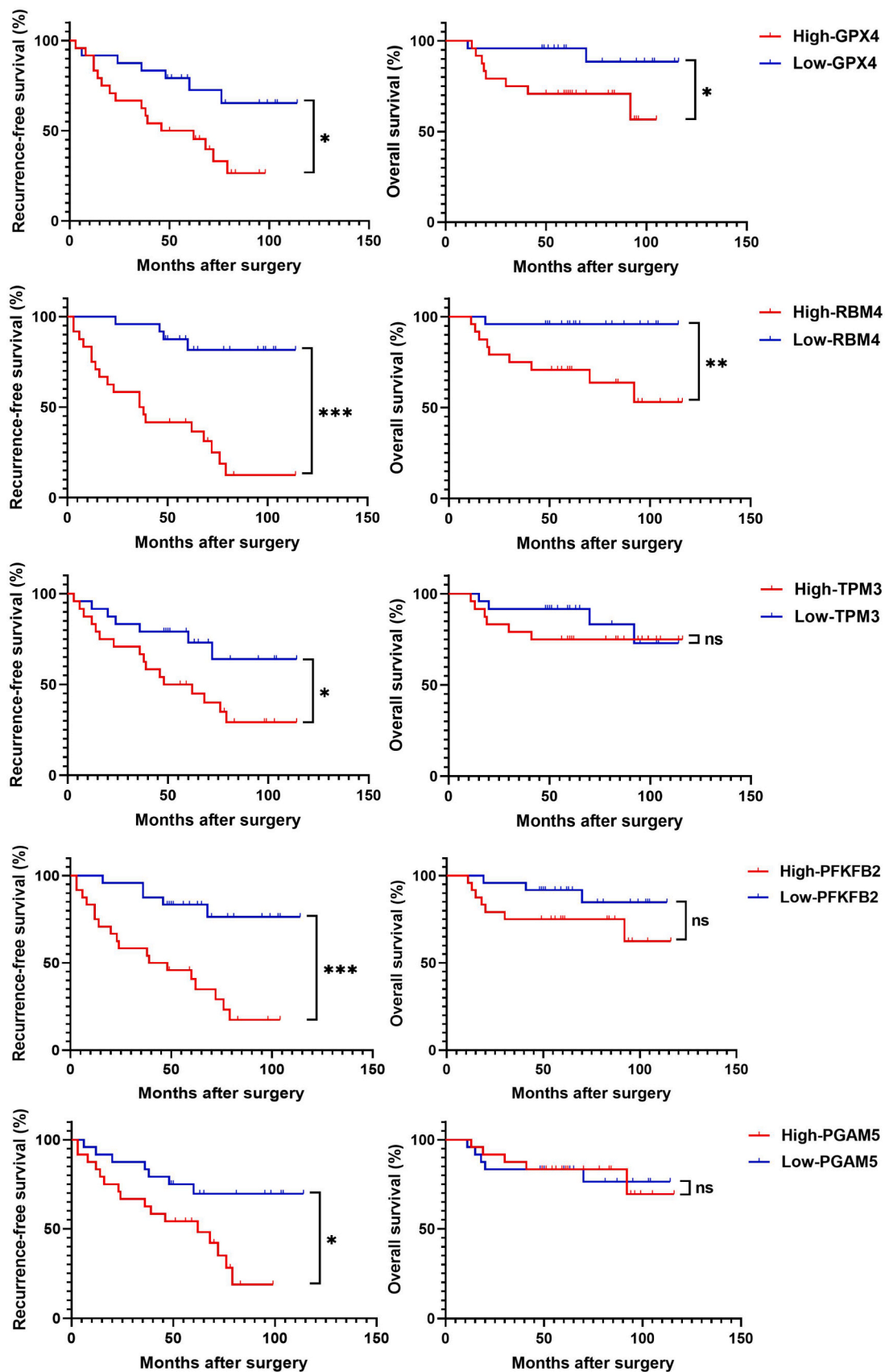


**Fig. 5.** The prognostic value of GPX4, RBM4, TPM3, PFKFB2, PGAM5 in 48 patients with GIST. Comparison of Recurrence-free survival (RFS) and overall survival (OS) between patients with high expressions of these five proteins and low expressing cases in GIST via Kaplan-Meier analysis. (\* $P < 0.05$ , \*\* $P < 0.01$ , \*\*\* $P < 0.001$ ).

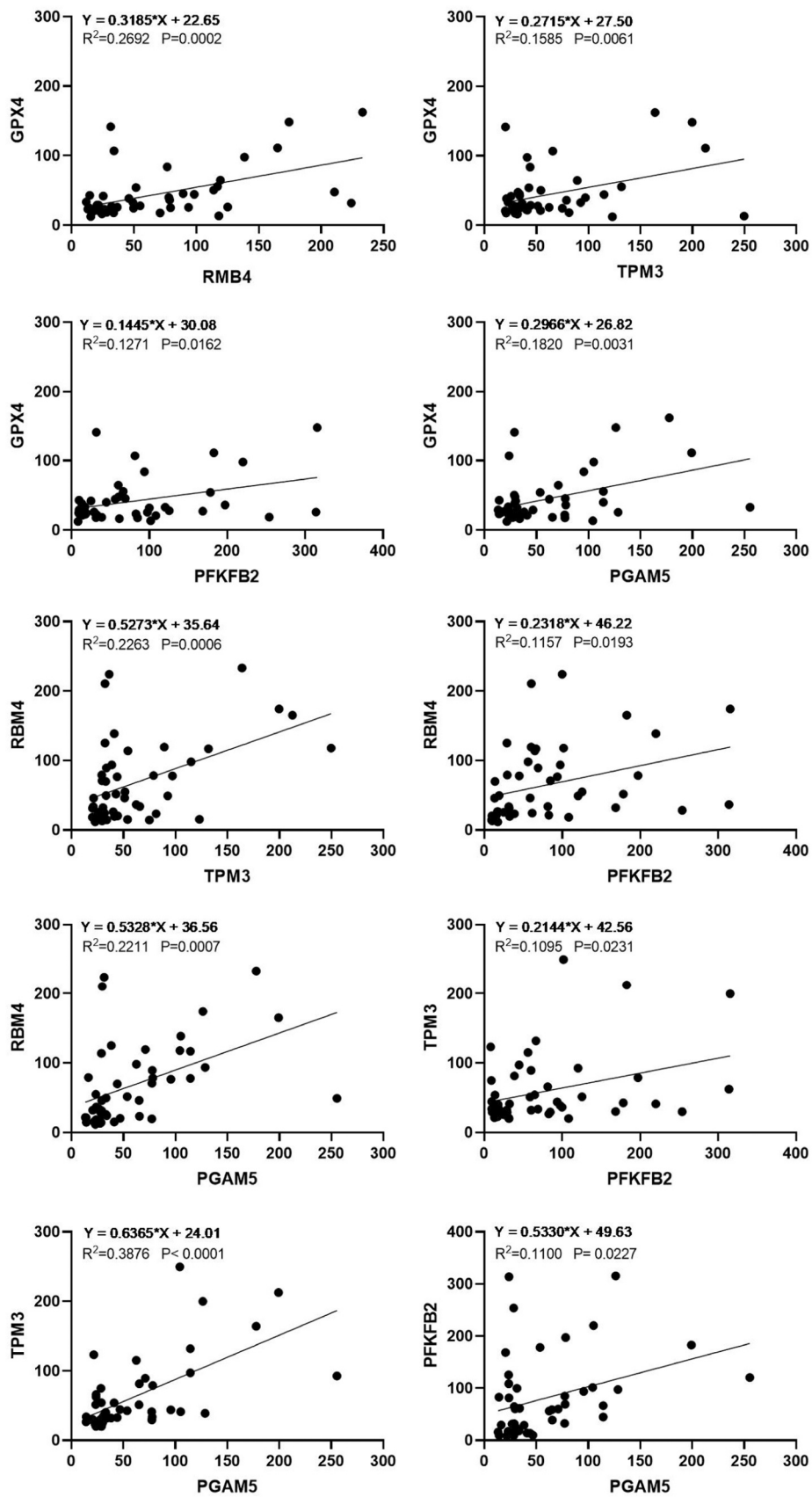


**Fig. 6.** Interrelationships of 5 Proteins in Predicting GIST Recurrence. Pearson regression analysis was performed to assess the correlation between the integrated optical density (IOD) levels of the five proteins among the 48 included GIST patients.

**Table 2**  
Correlations between GPX4/RBM4/TPM3/PFKFB2/PGAM5 expressions and clinical features.

	GPX4		RBM4		TPM3		PFKFB2		PGAM5	
	High	Low	High	Low	High	Low	High	Low	High	Low
No.	24	24	24	24	24	24	24	24	24	24
Age (years)	57.67 ± 11.18	58.58 ± 11.88	58.71 ± 11.06	57.54 ± 11.98	57.29 ± 12.05	58.96 ± 10.95	59.21 ± 11.27	57.04 ± 11.71	57.33 ± 10.64	58.92 ± 12.33
BMI (kg/m <sup>2</sup> )	23.24 ± 2.76	23.68 ± 3.68	23.28 ± 2.78	23.64 ± 3.67	23.83 ± 3.58	23.09 ± 2.85	23.36 ± 3.14	23.56 ± 3.37	24.07 ± 3.31	22.85 ± 3.08
Inpatient days	13.83 ± 5.13	13.71 ± 4.67	15.04 ± 5.10	12.50 ± 4.32	14.71 ± 5.70	12.83 ± 3.71	14.33 ± 5.00	13.21 ± 4.74	13.79 ± 4.49	13.75 ± 5.29
RFS (month)	<b>48.04</b> ± <b>29.70</b>	<b>66.58</b> ± <b>32.54</b> *	<b>41.67</b> ± <b>31.08</b>	<b>72.96</b> ± <b>25.37***</b>	52.67 ± 33.90	61.96 ± 30.44	<b>43.83</b> ± <b>31.42</b>	<b>70.79</b> ± <b>27.47**</b>	<b>47.33</b> ± <b>28.73</b>	<b>67.29</b> ± <b>32.97</b> *
OS (month)	<b>59.67</b> ± <b>28.79</b>	<b>76.50</b> ± <b>28.65</b> *	61.38 ± 32.39	74.79 ± 25.59	66.83 ± 32.50	69.33 ± 27.17	61.42 ± 31.94	74.75 ± 26.17	66.08 ± 26.56	70.08 ± 32.92
Sex										
Males	15 (62.50 %)	18 (75.00 %)	<b>13 (54.17 %)</b>	<b>20 (83.33 %)</b>	16 (66.67 %)	17 (70.83 %)	17 (70.83 %)	16 (66.67 %)	14 (58.33 %)	19 (79.17 %)
Females	9 (37.50 %)	6 (25.00 %)	<b>11 (45.83 %)</b>	<b>4 (16.67 %)*</b>	8 (33.33 %)	7 (29.17 %)	7 (29.17 %)	8 (33.33 %)	10 (41.67 %)	5 (20.83 %)
Surgery way										
Laparotomy	18 (75.00 %)	14 (58.33 %)	16 (66.67 %)	16 (66.67 %)	16 (66.67 %)	16 (66.67 %)	14 (58.33 %)	18 (75.00 %)	17 (70.83 %)	15 (62.50 %)
Laparoscopy	6 (25.00 %)	10 (41.67 %)	8 (33.33 %)	8 (33.33 %)	8 (33.33 %)	8 (33.33 %)	10 (41.67 %)	6 (25.00 %)	7 (29.17 %)	9 (37.50 %)
Tumor size (cm)										
> 2, ≤ 5	4 (16.67 %)	6 (25.00 %)	4 (16.67 %)	6 (25.00 %)	7 (29.17 %)	3 (12.50 %)	6 (25.00 %)	4 (16.67 %)	4 (16.67 %)	6 (25.00 %)
> 5, ≤ 10	10 (41.67 %)	11 (45.83 %)	11 (45.83 %)	10 (41.67 %)	8 (33.33 %)	13 (54.17 %)	11 (45.83 %)	10 (41.67 %)	12 (50.00 %)	9 (37.50 %)
> 10	10 (41.67 %)	7 (29.17 %)	9 (37.50 %)	8 (33.33 %)	9 (37.50 %)	8 (33.33 %)	7 (29.17 %)	10 (41.67 %)	8 (33.33 %)	9 (37.50 %)
Tumor site										
Gastric	10 (41.67 %)	9 (37.50 %)	11 (45.83 %)	8 (33.33 %)	9 (37.50 %)	10 (41.67 %)	11 (45.83 %)	8 (33.33 %)	8 (33.33 %)	11 (45.83 %)
Non-gastric	14 (58.33 %)	15 (62.50 %)	13 (54.17 %)	16 (66.67 %)	15 (62.50 %)	14 (58.33 %)	13 (54.17 %)	16 (66.67 %)	16 (66.67 %)	13 (54.17 %)
Mitotic index (/50 FP)										
≤ 5	8 (33.33 %)	12 (50.00 %)	8 (33.33 %)	12 (50.00 %)	9 (37.50 %)	11 (45.83 %)	9 (37.50 %)	11 (45.83 %)	10 (41.67 %)	10 (41.67 %)
> 5	16 (66.67 %)	12 (50.00 %)	16 (66.67 %)	12 (50.00 %)	15 (62.50 %)	13 (54.17 %)	15 (62.50 %)	13 (54.17 %)	14 (58.33 %)	14 (58.33 %)
Recurrence risk										
High	19 (79.17 %)	18 (75.00 %)	19 (79.17 %)	18 (75.00 %)	19 (79.17 %)	18 (75.00 %)	19 (79.17 %)	18 (75.00 %)	20 (83.33 %)	17 (70.83 %)
Medium	4 (16.67 %)	3 (12.50 %)	4 (16.67 %)	3 (12.50 %)	3 (12.50 %)	4 (16.67 %)	3 (12.50 %)	4 (16.67 %)	3 (12.50 %)	4 (16.67 %)
Low	1 (4.17 %)	3 (12.50 %)	1 (4.17 %)	3 (12.50 %)	2 (8.33 %)	2 (8.33 %)	2 (8.33 %)	2 (8.33 %)	1 (4.17 %)	3 (12.50 %)
Death										
Yes	<b>16 (66.67 %)</b>	<b>22 (91.67 %)</b>	<b>15 (62.50 %)</b>	<b>23 (95.83 %)</b>	18 (75.00 %)	20 (83.33 %)	17 (70.83 %)	21 (87.50 %)	19 (79.17 %)	19 (79.17 %)
No	<b>8 (33.33 %)</b>	<b>2 (8.33 %)</b> *	<b>9 (37.50 %)</b>	<b>1 (4.17 %)**</b>	6 (25.00 %)	4 (16.67 %)	7 (29.17 %)	3 (12.50 %)	5 (20.83 %)	5 (20.83 %)
Recurrence										
Yes	<b>16 (66.67 %)</b>	<b>7 (29.17 %)</b>	<b>19 (79.17 %)</b>	<b>4 (16.67 %)</b>	<b>16 (66.67 %)</b>	<b>7 (29.17 %)</b>	<b>18 (75.00 %)</b>	<b>5 (20.83 %)</b>	<b>16 (66.67 %)</b>	<b>7 (29.17 %)</b>
No	<b>8 (33.33 %)</b>	<b>17 (70.83 %)**</b>	<b>5 (20.83 %)</b>	<b>20 (83.33 %)**</b>	<b>8 (33.33 %)</b>	<b>17 (70.83 %)**</b>	<b>6 (25.00 %)</b>	<b>19 (79.17 %)**</b>	<b>8 (33.33 %)</b>	<b>17 (70.83 %)**</b>
IOD of GPX4										
High	-	-	<b>17 (70.83 %)</b>	<b>7 (29.17 %)</b>	15 (62.50 %)	9 (37.50 %)	14 (58.33 %)	10 (41.67 %)	15 (62.50 %)	9 (37.50 %)
Low	-	-	<b>7 (29.17 %)</b>	<b>17 (70.83 %)**</b>	9 (37.50 %)	15 (62.50 %)	10 (41.67 %)	14 (58.33 %)	9 (37.50 %)	15 (62.50 %)
IOD of RBM4										
High	<b>17 (70.83 %)</b>	<b>7 (29.17 %)</b>	-	-	15 (62.50 %)	9 (37.50 %)	<b>17 (70.83 %)</b>	<b>7 (29.17 %)</b>	<b>18 (75.00 %)</b>	<b>6 (25.00 %)</b>
Low	<b>7 (29.17 %)</b>	<b>17 (70.83 %)**</b>	-	-	9 (37.50 %)	15 (62.50 %)	<b>7 (29.17 %)</b>	<b>17 (70.83 %)**</b>	<b>6 (25.00 %)</b>	<b>18 (75.00 %)**</b>
IOD of TPM3										
High	15 (62.50 %)	9 (37.50 %)	15 (62.50 %)	9 (37.50 %)	-	-	14 (58.33 %)	10 (41.67 %)	<b>18 (75.00 %)</b>	<b>6 (25.00 %)</b>
Low	9 (37.50 %)	15 (62.50 %)	9 (37.50 %)	15 (62.50 %)	-	-	10 (41.67 %)	14 (58.33 %)	<b>6 (25.00 %)</b>	<b>18 (75.00 %)**</b>
IOD of PFKFB2										
High	14 (58.33 %)	10 (41.67 %)	<b>17 (70.83 %)</b>	<b>7 (29.17 %)</b>	14 (58.33 %)	10 (41.67 %)	-	-	14 (58.33 %)	10 (41.67 %)

(continued on next page)

Table 2 (continued)

	GPX4		RBM4		TPM3		PFKFB2		PGAM5	
	High	Low	High	Low	High	Low	High	Low	High	Low
Low	10 (41.67 %)	14 (58.33 %)	7 (29.17 %)	17 (70.83 %)**	10 (41.67 %)	14 (58.33 %)	-	-	10 (41.67 %)	14 (58.33 %)
IOD of PGAM5										
High	15 (62.50 %)	9 (37.50 %)	18 (75.00 %)	6 (25.00 %)	18 (75.00 %)	6 (25.00 %)	14 (58.33 %)	10 (41.67 %)	-	-
Low	9 (37.50 %)	15 (62.50 %)	6 (25.00 %)	18 (75.00 %)**	6 (25.00 %)	18 (75.00 %)**	10 (41.67 %)	14 (58.33 %)	-	-

Statistical significance was determined by t-test and chi-square test. (\*P < 0.05, \*\*P < 0.01, \*\*\*P < 0.001).

established that PGAM5 expression is associated with necroptosis [53, 54] and mitophagy [55,56]. In cancers, PGAM5 levels are significantly higher in lung cancer tissues than in normal tissues [57] and its depletion inhibits cell growth and promotes apoptosis in HCC [58]. What's more, Zhong et al. showed significant PGAM5 upregulation in tumor versus normal liver tissues, with HCC patients having higher PGAM5 levels facing worse OS and RFS [59], paralleling our findings on PGAM5 and GIST. However, other studies have not identified a direct relationship between PGAM5 and GIST.

Overall, identifying high-risk patients for timely treatment and rigorous follow-up using these five biomarkers could significantly extend GIST patients' survival. However, the limitations of this study are also worth mentioning: targeted MS approaches, like selected reaction monitoring proteomics analysis, should follow as a distinct verification phase after identifying differentially expressed proteins; Larger prospective studies are needed to validate these biomarkers' clinical utility and integration into current risk assessment models. Additionally, understanding how these biomarkers contribute to GIST recurrence could reveal new therapeutic targets and personalized strategies for GIST management. Exploring these biomarkers in GIST patients' blood and urine is crucial for developing non-invasive detection and monitoring methods.

## 5. Conclusion

Our study identified five biomarkers—GPX4, RBM4, TPM3, PFKFB2, and PGAM5—that are clinically significant in predicting GIST recurrence. Elevated expressions of these biomarkers in GIST tissues correlate with poorer RFS and OS. These biomarkers show great potential as prognostic indicators for GIST recurrence, facilitating early intervention and enhancing patient outcomes.

## Ethics approval and consent to participate

The present study was approved by the Institutional Review Board of Peking Union Medical College Hospital. The ethical approval code of this study is No: K22C0484.

## Fundings

This study was funded by the National High Level Hospital Clinical Research Funding (2022-PUMCH-C-048, 2022-PUMCH-B-005, 2022-PUMCH-A-051), Beijing Natural Science Foundation (7232117), Beijing Medical Award Foundation (YXJL-2021-0838-0761), Bethune Charitable Foundation (WCJZL202106), Wu Jieping Medical Foundation (320.6750.2022-10-1) and Beijing Xisike Clinical Oncology Research Foundation (Y-NESTLE2022ZD-0105).

## Author contributions

The study was conceived and designed by Juan Sun and Weiming Kang. Experiments were conducted by Juan Sun and Jie Li. Juan Sun wrote the manuscript. Yixuan He, Xin Ye collected the clinical data. Juan

Sun and Jie Li analyzed data. Weiming Kang and Xin Ye supervised the overall research, secured funding, and interpreted results.

## Competing interests

The authors have declared that no competing interest exists.

## Declaration of Competing Interest

The authors declare that they have no known competing financial interests or personal relationships that could have appeared to influence the work reported in this paper.

## Appendix A. Supporting information

Supplementary data associated with this article can be found in the online version at doi:10.1016/j.csbj.2024.02.017.

## References

- [1] Blay JY, Kang YK, Nishida T, von Mehren M. Gastrointestinal stromal tumours. *Nat Rev Dis Prim* 2021;7(1):22.
- [2] Khan TM, Verbus EA, Rossi AJ, et al. Patient demographics, clinicopathologic features, and outcomes in wild-type gastrointestinal stromal tumor: a national cohort analysis. *Sci Rep* 2022;12(1):5774.
- [3] Klug LR, Khosroyani HM, Kent JD, Heinrich MC. New treatment strategies for advanced-stage gastrointestinal stromal tumours. *Nat Rev Clin Oncol* 2022;19(5):328–41.
- [4] Lin JX, Wang FH, Wang ZK, et al. Prediction of the mitotic index and preoperative risk stratification of gastrointestinal stromal tumors with CT radiomic features. *La Radiol Med* 2023;128(6):644–54.
- [5] Casali PG, Abecassis N, Aro HT, et al. Gastrointestinal stromal tumours: ESMO-EURACAN clinical practice guidelines for diagnosis, treatment and follow-up. *Ann Oncol: J Eur Soc Med Oncol* 2018;29(Suppl 4):iv267.
- [6] von Mehren M, Randall RL, Benjamin RS, et al. Gastrointestinal stromal tumors, version 2.2014. *J Natl Compr Cancer Netw: JNCCN* 2014;12(6):853–62.
- [7] Miettinen M, Lasota J. Gastrointestinal stromal tumors: pathology and prognosis at different sites. *Semin Diagn Pathol* 2006;23(2):70–83.
- [8] Casali PG, Abecassis N, Aro HT, et al. Gastrointestinal stromal tumours: ESMO-EURACAN Clinical Practice Guidelines for diagnosis, treatment and follow-up. *Ann Oncol: J Eur Soc Med Oncol* 2018;29(Suppl 4):iv68–78.
- [9] Bleckman RF, Roets E, NS LJ, et al. Local recurrence in primary localised resected gastrointestinal stromal tumours: a registry observational national cohort study including 912 patients. *Eur J Cancer (Oxf, Engl)* 1990;2023;186:113–21.
- [10] von Mehren M, Randall RL, Benjamin RS, et al. Soft tissue sarcoma, version 2.2018, NCCN clinical practice guidelines in oncology. *J Natl Compr Cancer Netw: JNCCN* 2018;16(5):536–63.
- [11] Fletcher CD, Berman JJ, Corless C, et al. Diagnosis of gastrointestinal stromal tumors: A consensus approach. *Hum Pathol* 2002;33(5):459–65.
- [12] Dematteo RP, Ballman KV, Antonescu CR, et al. Adjuvant imatinib mesylate after resection of localised, primary gastrointestinal stromal tumour: a randomised, double-blind, placebo-controlled trial. *Lancet (Lond, Engl)* 2009;373(9669):1097–104.
- [13] Mao X, Yang X, Chen X, et al. Single-cell transcriptome analysis revealed the heterogeneity and microenvironment of gastrointestinal stromal tumors. *Cancer Sci* 2021;112(3):1262–74.
- [14] Rutkowski P. Why we still need the better risk classification for GIST. *Ann Surg Oncol* 2021;28(5):2425–7.
- [15] Lu X, Pang Y, Cao H, et al. Integrated screens identify CDK1 as a therapeutic target in advanced gastrointestinal stromal tumors. *Cancer Res* 2021;81(9):2481–94.
- [16] Yu JE, Yeo IJ, Yoo SS, et al. Induction of ER stress-mediated apoptosis through SOD1 upregulation by deficiency of CH13L1 inhibits lung metastasis. *Theranostics* 2023;13(8):2693–709.

- [17] Gronchi A, Judson I, Nishida T, et al. Adjuvant treatment of GIST with imatinib: solid ground or still quicksand? A comment on behalf of the EORTC Soft Tissue and Bone Sarcoma Group, the Italian Sarcoma Group, the NCRI Sarcoma Clinical Studies Group (UK), the Japanese Study Group on GIST, the French Sarcoma Group and the Spanish Sarcoma Group (GEIS). *Eur J Cancer (Oxf, Engl: 1990)* 2009;45(7):1103–6.
- [18] Trinh VQ, Dashti NK, Cates JMM. A proposed risk assessment score for gastrointestinal stromal tumors based on evaluation of 19,030 cases from the National Cancer Database. *J Gastroenterol* 2021;56(11):964–75.
- [19] Kim JY, Kim TJ, Lee DK, et al. A preoperative risk prediction model for high malignancy potential gastrointestinal stromal tumors of the stomach. *Surg Endosc* 2022;36(3):2129–37.
- [20] Forcina GC, Dixon SJ. GPX4 at the crossroads of lipid homeostasis and ferroptosis. *Proteomics* 2019;19(18):e1800311.
- [21] Dixon SJ, Lemberg KM, Lamprecht MR, et al. Ferroptosis: an iron-dependent form of nonapoptotic cell death. *Cell* 2012;149(5):1060–72.
- [22] Chen X, Kang R, Kroemer G, Tang D. Broadening horizons: the role of ferroptosis in cancer. *Nat Rev Clin Oncol* 2021;18(5):280–96.
- [23] Pohl S, Pervaiz S, Dharmarajan A, Agostino M. Gene expression analysis of heat-shock proteins and redox regulators reveals combinatorial prognostic markers in carcinomas of the gastrointestinal tract. *Redox Biol* 2019;25:101060.
- [24] Lu Y, Qin H, Jiang B, et al. KLF2 inhibits cancer cell migration and invasion by regulating ferroptosis through GPX4 in clear cell renal cell carcinoma. *Cancer Lett* 2021;522:1–13.
- [25] Ishida T, Takahashi T, Kurokawa Y, et al. Targeted therapy for drug-tolerant persister cells after imatinib treatment for gastrointestinal stromal tumours. *Br J Cancer* 2021;125(11):1511–22.
- [26] Delvaux M, Hagué P, Craciun L, et al. Ferroptosis induction and YAP inhibition as new therapeutic targets in gastrointestinal stromal tumors (GISTs). *Cancers* 2022;14(20).
- [27] Lin JC, Tarn WY. RNA-binding motif protein 4 translocates to cytoplasmic granules and suppresses translation via argonaute2 during muscle cell differentiation. *J Biol Chem* 2009;284(50):34658–65.
- [28] Bartkova J, Rezaei N, Liontos M, et al. Oncogene-induced senescence is part of the tumorigenesis barrier imposed by DNA damage checkpoints. *Nature* 2006;444(7119):633–7.
- [29] Lee S, Schmitt CA. The dynamic nature of senescence in cancer. *Nat Cell Biol* 2019;21(1):94–101.
- [30] Estévez-García IO, Cordoba-Gonzalez V, Lara-Padilla E, et al. Glucose and glutamine metabolism control by APC and SCF during the G1-to-S phase transition of the cell cycle. *J Physiol Biochem* 2014;70(2):569–81.
- [31] Ahn E, Kumar P, Mukha D, Tzur A, Shlomi T. Temporal fluxomics reveals oscillations in TCA cycle flux throughout the mammalian cell cycle. *Mol Syst Biol* 2017;13(11):953.
- [32] Chen L, Zhang W, Chen D, et al. RBM4 dictates ESCC cell fate switch from cellular senescence to glutamine-addiction survival through inhibiting LKB1-AMPK-axis. *Signal Transduct Target Ther* 2023;8(1):159.
- [33] Han H, Lin T, Wang Z, et al. RNA-binding motif 4 promotes angiogenesis in HCC by selectively activating VEGF-A expression. *Pharmacol Res* 2023;187:106593.
- [34] Lin JC, Lin CY, Tarn WY, Li FY. Elevated SRPK1 lessens apoptosis in breast cancer cells through RBM4-regulated splicing events. *RNA (N Y, NY)* 2014;20(10):1621–31.
- [35] Qi Y, Yu J, Han W, et al. A splicing isoform of TEAD4 attenuates the Hippo-YAP signalling to inhibit tumour proliferation. *Nat Commun* 2016;7:ncmms11840.
- [36] Chen JY, Liu LP, Xu JF. Decrease of RBM4 indicates poor prognosis in patients with hepatocellular carcinoma after hepatectomy. *Oncotargets Ther* 2017;10:339–45.
- [37] Pieples K, Arteaga G, Solaro RJ, et al. Tropomyosin 3 expression leads to hypercontractility and attenuates myofilament length-dependent Ca(2+) activation. *Am J Physiol Heart Circ Physiol* 2002;283(4):H1344–53.
- [38] Greco A, Miranda C, Pierotti MA. Rearrangements of NTRK1 gene in papillary thyroid carcinoma. *Mol Cell Endocrinol* 2010;321(1):44–9.
- [39] Li Z, Yang R, Zhao J, et al. Molecular diagnosis and targeted therapy of a pediatric chronic eosinophilic leukemia patient carrying TPM3-PDGFRB fusion. *Pediatr Blood Cancer* 2011;56(3):463–6.
- [40] Yu SB, Gao Q, Lin WW, Kang MQ. Proteomic analysis indicates the importance of TPM3 in esophageal squamous cell carcinoma invasion and metastasis. *Mol Med Rep* 2017;15(3):1236–42.
- [41] Choi HS, Yim SH, Xu HD, et al. Tropomyosin3 overexpression and a potential link to epithelial-mesenchymal transition in human hepatocellular carcinoma. *BMC Cancer* 2010;10:122.
- [42] Tao T, Shi Y, Han D, et al. TPM3, a strong prognosis predictor, is involved in malignant progression through MMP family members and EMT-like activators in gliomas. *Tumour Biol: J Int Soc Oncodev Biol Med* 2014;35(9):9053–9.
- [43] Atiq MA, Davis JL, Hornick JL, et al. Mesenchymal tumors of the gastrointestinal tract with NTRK rearrangements: a clinicopathological, immunophenotypic, and molecular study of eight cases, emphasizing their distinction from gastrointestinal stromal tumor (GIST). *Mod Pathol: J U S Can Acad Pathol, Inc* 2021;34(1):95–103.
- [44] Huang WK, Huang SC, Chen CM, et al. Marked response to larotrectinib in pelvic spindle cell sarcoma with concurrent TPM3-NTRK1 fusion and CDK4/MDM2 amplification: a case report. *JCO Precis Oncol* 2023;(7):e2200528.
- [45] Tang N, Zhang J, Fu X, Xie W, Qiu Y. PP2A $\alpha$  inhibits PFKFB2-induced glycolysis to promote termination of liver regeneration. *Biochem Biophys Res Commun* 2020;526(1):1–7.
- [46] Cairns RA, Harris IS, Mak TW. Regulation of cancer cell metabolism. *Nat Rev Cancer* 2011;11(2):85–95.
- [47] Orang AV, Petersen J, McKinnon RA, Michael MZ. Micromanaging aerobic respiration and glycolysis in cancer cells. *Mol Metab* 2019;23:98–126.
- [48] Vander Heiden MG, Cantley LC, Thompson CB. Understanding the Warburg effect: the metabolic requirements of cell proliferation. *Sciences (N Y, NY)* 2009;324(5930):1029–33.
- [49] Qu J, Yang J, Chen M, Wei R, Tian J. CircFLNA acts as a sponge of miR-646 to facilitate the proliferation, metastasis, glycolysis, and apoptosis inhibition of gastric cancer by targeting PFKFB2. *Cancer Manag Res* 2020;12:8093–103.
- [50] Ji D, Lu ZT, Li YQ, et al. MACC1 expression correlates with PFKFB2 and survival in hepatocellular carcinoma. *Asian Pac J Cancer Prev: APJCP* 2014;15(2):999–1003.
- [51] Zhao L, Ji G, Le X, et al. Long noncoding RNA LINC00092 acts in cancer-associated fibroblasts to drive glycolysis and progression of ovarian cancer. *Cancer Res* 2017;77(6):1369–82.
- [52] Lo SC, Hannink M. PGAM5 tethers a ternary complex containing Keap1 and Nrf2 to mitochondria. *Exp Cell Res* 2008;314(8):1789–803.
- [53] Wang YS, Yu P, Wang Y, et al. AMP-activated protein kinase protects against necroptosis via regulation of Keap1-PGAM5 complex. *Int J Cardiol* 2018;259:153–62.
- [54] Dong XH, Liu H, Zhang MZ, et al. Postconditioning with inhaled hydrogen attenuates skin ischemia/reperfusion injury through the RIP-MLKL-PGAM5/Drp1 necrotic pathway. *Am J Transl Res* 2019;11(1):499–508.
- [55] Chen G, Han Z, Feng D, et al. A regulatory signaling loop comprising the PGAM5 phosphatase and CK2 controls receptor-mediated mitophagy. *Mol Cell* 2014;54(3):362–77.
- [56] Lu W, Sun J, Yoon JS, et al. Mitochondrial protein PGAM5 regulates mitophagic protection against cell necroptosis. *PLoS One* 2016;11(1):e0147792.
- [57] Ng Kee Kwong F, Nicholson AG, Pavlidis S, Adcock IM, Chung KF. PGAM5 expression and macrophage signatures in non-small cell lung cancer associated with chronic obstructive pulmonary disease (COPD). *BMC Cancer* 2018;18(1):1238.
- [58] Cheng J, Qian D, Ding X, et al. High PGAM5 expression induces chemoresistance by enhancing Bcl-xL-mediated anti-apoptotic signaling and predicts poor prognosis in hepatocellular carcinoma patients. *Cell Death Dis* 2018;9(10):991.
- [59] Zhong C, Niu Y, Liu W, et al. S100A9 derived from chemoembolization-induced hypoxia governs mitochondrial function in hepatocellular carcinoma progression. *Adv Sci (Weinh, Baden-Wurt, Ger)* 2022;9(30):e2202206.